Coupling a rebuild shuttle system with biosynthetic pathway and transcription factor engineering for enhanced L-cysteine production

Zhang et al.

Supplementary Method 1. Purification of CysB protein.

The histidine tag in the recombinant plasmid pET-28a (+)-CysB can chelate with the bivalent Ni^{2+} in the nickel column and carry on the affinity chromatography to the protein. The specific steps are as follows:

(1) clean the pipeline with PBS for 4-5 min minutes before adding the nickel column, and clean the import of the protein purifier.

(2) after the baseline was flattened with PBS, the protein supernatant samples that passed through the membrane were injected into the column through the injection port of the purifier, and after injection, the baseline was flushed out with PBS.

(3) rinse the miscellaneous proteins with 50 mM imidazole, flush the baseline with PBS, then separate the target protein with 500 mM imidazole after the baseline is stable, and collect the target protein according to the displayed UV value. The SDS-PAGE verification of the target protein can be used in the experiment if the purity is more than 90%.

Supplementary Method 2. Determination of affinity between CysB protein and DNA by Fortebio.

(1) preparation of Fortebio experimental samples.

DNA: synthesis of double-stranded DNA with biotin tag at 5 'end.

Purpose protein: purity more than 90%, concentration more than 1 mg/L.

Experimental chip: SA chip (which can specifically capture substances with biological tags) was used.

(2) Fortebio experiment steps Firstly, the probe was pre-wet in PBST solution, and the DNA and the protein were diluted. The protein was diluted to 10 μM as the highest concentration and 2 times gradient dilution. The sample plate is set up according to the actual position of the sample in plate definition. According to the needs of multi-concentration complete kinetic analysis, the analysis steps need baseline1 (for leveling the baseline, usually 60 s), loading (for curing DNA, usually 300 s), baseline2 (for leveling the baseline, usually 300 s), association (for DNA binding to protein, usually 180 s), and dissociation (for dissociation of DNA and protein, usually 300 s). Dissociate the double-stranded DNA with 5m NaCl) five steps. Therefore, you need to set up four columns of samples, namely buffer1 for the baseline1 step, load for the loading step, buffer2 for the baseline2 and dissociation steps, and sample for the association step.

Supplementary Method 3. The relevant indicators of the GCB2 strain in a 5 L fermenter.

The total input for the GCB2 strain in a 5 L fermenter (including the basal medium and Supplement bottle 1) consisted of: 20 g of ammonium sulfate, 26 g of sodium thiosulfate, 11.5 g of ammonium thiosulfate, and 570 g of glucose. After fermentation, a total of 2 L of fermentation broth was collected, yielding 71.08 g of L-cysteine. The total moles of sulfur atoms in the input were 0.635 M, and the output contained 0.587 M of sulfur atoms, resulting in a sulfur assimilation rate of 92.44%. The glucose-to-cysteine conversion efficiency was 0.125 g/g.

Supplementary Result 1. The impact of protein scaffold ligand and enzyme fusion on biological function.

Studies have shown that the fusion expression of protein scaffold ligands and pathway enzymes CysK, CysM and NrdH did not cause significant spatial structure changes, and the protein scaffold ligands were always exposed on the outside of the structure (Supplementary Fig. 6, 7, 9). However, when the protein scaffold ligand is fused to the C-terminus of CysE, the ligand is not free outside the multimeric structure but is embedded inside. Obviously, the protein scaffold ligand cannot interact with the corresponding domain due to steric hindrance. The combination of effects makes it impossible to achieve co-localization assembly of pathway enzymes (Supplementary Fig. 7c). And the protein scaffold ligand PDZ lig embedded inside the CysE hexamer may affect the original structure of CysE, thereby affecting its biological function. The protein scaffold ligand was then fused to the N-terminus of CysE. At this time, the protein scaffold ligand was completely exposed outside the hexamer structure, and the biological function of the cysE protein was not affected (Supplementary Fig. 8,9).

Supplementary Result 2. EMSA experiments confirm the regulation of genes by the CysB protein.

Using Supplementary Method 1, we purified the CysB proteins (wild-type and the V122G mutant). The purity (>90%) was confirmed by SDS-PAGE, followed by electrophoretic mobility shift assays (EMSA). DNA fragments are negatively charged and migrate from the negative to the positive electrode during electrophoresis; under identical conditions, their migration distance is inversely proportional to their molecular weight. After incubating proteins with DNA, the molecular weight of the DNA fragments bound to proteins increases, causing a slower migration during electrophoresis. By staining with SYBR Green, bands with different mobilities can be observed.

O-acetyl-L-serine (OAS) and its isomer N-acetylserine (NAS)—OAS spontaneously isomerized to NAS under alkaline and physiological conditions—have multiple effects on CysB in vitro, including transcriptional activation, altering DNA-binding affinity, and modulating the DNA bending angle after CysB binding. OAS and NAS can stimulate the transcription of CysB-dependent genes *cysJIH*, *cysK*, and *cysP*, and increase the binding affinity at activation sites CBS-JI, CBS-K1, and CBS-P1.[1,2] By analyzing the mobility shifts in EMSA, the binding state between CysB and DNA can be inferred. Observing the intensity and migration rates of the bands representing CysB bound to the target gene and free DNA allows for a preliminary characterization of the binding properties between CysB and the target gene.

First, we optimized the concentrations of protein and DNA (using PcysK as an example). When the final concentrations were 0.1 μg protein and 1.5 μg DNA, the bound and free DNA bands could be clearly observed. Considering that OAS is an activator of CysB and sulfate is an inhibitor, we added both substances to the reaction system. Additionally, since thiosulfate is used as a sulfur source in L-cysteine production and its effect on CysB binding has not been reported, we included it in our study to investigate its role. Studies have shown that in the presence of NAS, the exogenous addition of 1 mM sodium sulfide can counteract the stimulatory effect of inducers on the CysB protein and the promoters *cysJIH*, *cysK*, and *cysPUWAM*.[3] Considering the interconversion between OAS and NAS, we added 10 mM OAS, 1 mM thiosulfate, and 1 mM sulfate to the reaction system to observe their effects on the binding bands.

Lane 1 contains free DNA; lanes 2, 3, 4, 5, 10, and 11 contain wild-type CysB; lanes 6, 7, 8, 9, 12, and 13 contain $CysB^{V122G}$. Since each lane includes 1.5 μg of DNA, we can preliminarily assess the binding of CysB to PcysK by comparing with the free DNA band. It was observed that after adding OAS, the free DNA band of CysB became significantly lighter (lane 4), but the inhibitory effects of sulfate and thiosulfate on CysB were not evident from the EMSA results (lanes 3 and 10). Moreover, compared with lane 4, the addition of OAS did not alleviate the inhibitory effects caused by sulfate and thiosulfate.

When CysB binds to PcysK, it induces a 100° bend in PcysK in the absence of OAS, and a 50° bend in the presence of OAS, resulting in the formation of "slow" (C1s) and "fast" (C1f) complexes, respectively. In the binding of $CysB^{V122G}$ to PcysK, C1f was clearly observed, and the free DNA band became significantly lighter, indicating that the mutant binds better to PcysK (lane 6). After adding OAS, the free DNA band in the $CysB^{V122G}$ - PcysK complex became even lighter (lane 8). The addition of sulfate and thiosulfate caused the free DNA band to become darker (lanes 7 and 13), but they did not inhibit the activation effect of OAS on $CysB^{V122G}$ (lanes 9 and 13). Additionally, a secondary complex (C2) band appeared in the binding of the mutant to PcysK, which may be due to the CysB tetramer having two different binding sites within PcysK.

In the EMSA experiments of the mutant, we found that thiosulfate may exert a repressive effect similar to that of sulfate on the binding between CysB and the target gene, affecting the protein-DNA interaction. For CysB, the repressive effects of sulfate or thiosulfate are not significantly alleviated by the addition of OAS. However, for $CysB^{V122G}$, the inhibitory effects caused by sulfate or thiosulfate can be ameliorated by adding OAS. Additionally, the complexes formed between the mutant and PcysK exhibited higher electrophoretic mobility compared to those with CysB. In all lanes where the mutant binds to PcysK, a clear "C2" band resulting from the mutant's binding to PcysK was observed. This may be due to the enhanced binding ability of the mutant protein to PcysK, leading to strong binding at two different binding sites within PcysK, thereby allowing the binding bands to be clearly visualized.

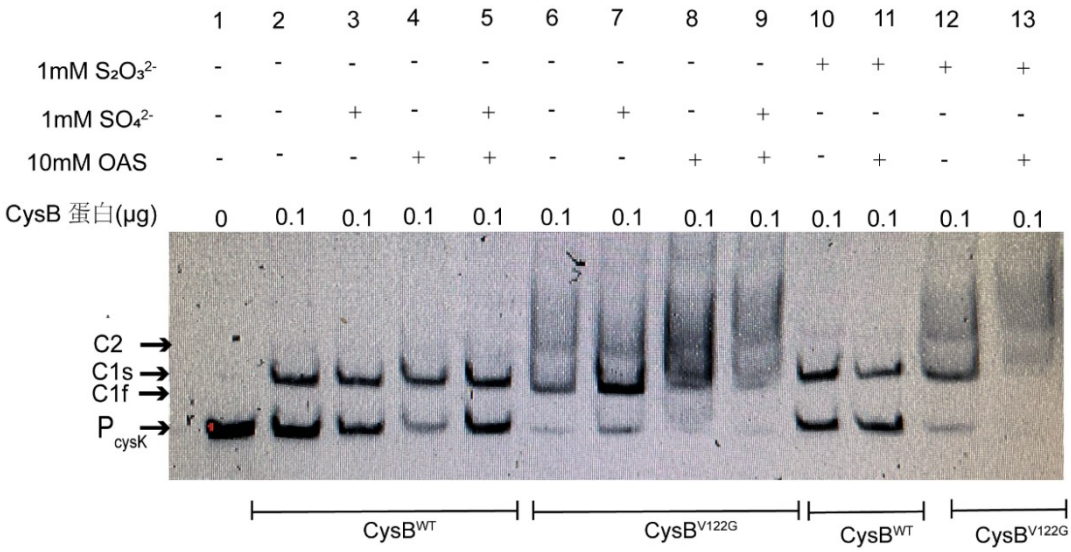

Fig. The binding of $CysB^{WT}$ and $CysB^{V122G}$ to target genes under different conditions was analyzed by EMSA assay.

1 only added PcysK (control)；2 added PcysK、0.1 μg $CysB^{WT}$；3 added PcysK、0.1 μg $CysB^{WT}$、1 mM Na_2SO_4；4 added PcysK、0.1 μg $CysB^{WT}$、10 mM OAS；5 added PcysK、0.1 μg $CysB^{WT}$、10 mM OAS、1 mM Na_2SO_4；6 added PcysK、0.1 μg $CysB^{V122G}$；7 added PcysK、0.1 μg $CysB^{V122G}$、1 mM Na_2SO_4；8 added PcysK、0.1 μg $CysB^{V122G}$、10 mM OAS；9 added PcysK、0.1 μg $CysB^{V122G}$、10 mM OAS、1 mM Na_2SO_4；10 added PcysK、0.1 μg $CysB^{WT}$、1 mM $Na_2S_2O_3$；11 added PcysK、0.1 μg $CysB^{WT}$、10 mM OAS、1 mM $Na_2S_2O_3$；12 added PcysK、0.1 μg CysBV122G、1 mM $Na_2S_2O_3$；13 added PcysK、0.1 μg $CysB^{V122G}$、10 mM OAS、1 mM $Na_2S_2O_3$、C2 represents the secondary complex band, C1f represents the fast primary complex band, and C1s represents the slow primary complex band.

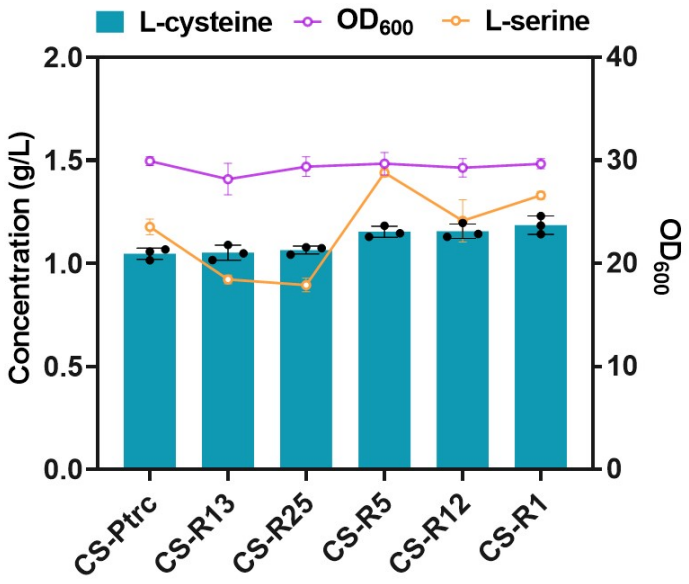

Supplementary Fig. 1. Impact of genomic integration of *cysE*^{f6} variants with varying expression strengths on strain production performance. Data are presented as mean values ± SD from three independent biological replicates (n = 3), the circles or squares represent individual data points. Source data are provided as a Source Data file.

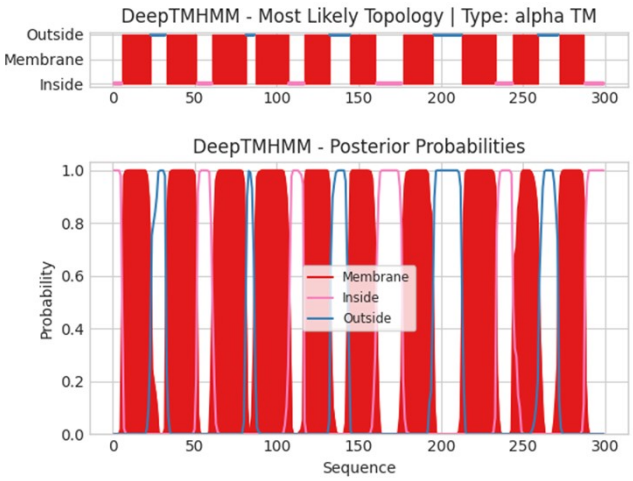

Supplementary Fig. 2. Transmembrane structure prediction of EamA.

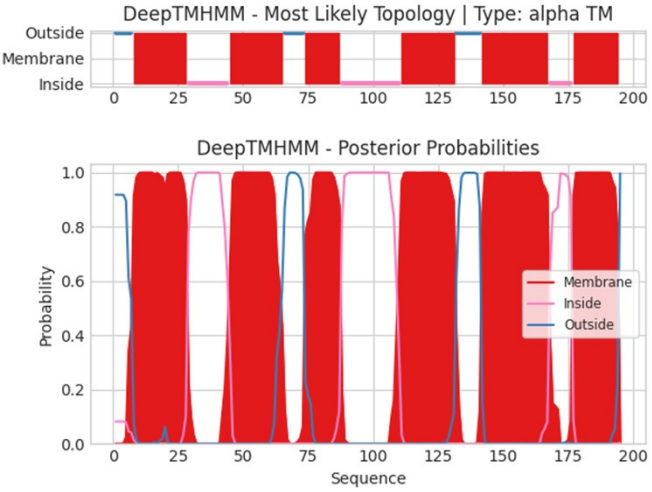

Supplementary Fig. 3. Transmembrane structure prediction of EamB.

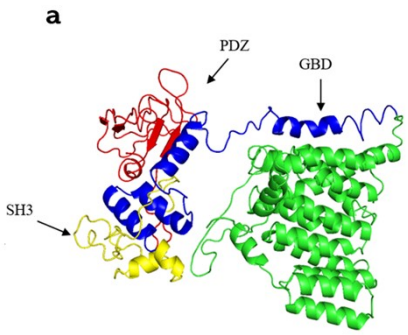

Supplementary Fig. 4. Protein scaffold domain GBD, SH3, PDZ superimposed on the C-terminal of EamA fusion protein structure simulation prediction results. Enzyme structure prediction diagram (**a**) EamA- GBD-SH3-PDZ (EamA C-terminal connection GBD-SH3-PDZ).

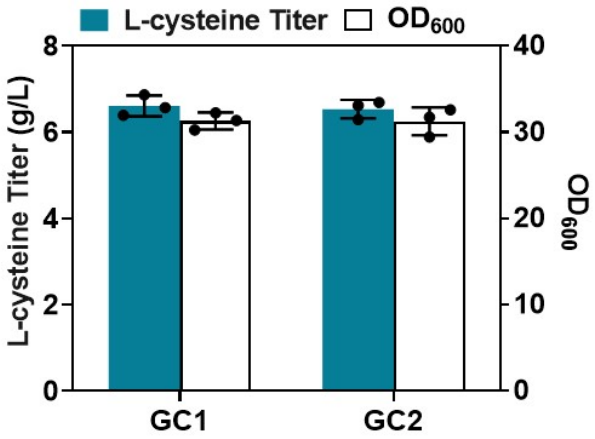

Supplementary Fig. 5. Effect of the protein scaffold domain on the channel protein EamA. GC2 (EamA-GBD-SH3-PDZ).

There was no significant difference in L-cysteine production between strains GC2 and GC1, and the superposition of three protein scaffold domains at the C-terminal of channel protein would not seriously affect the physiological function of EamA. These results laid a foundation for follow-up experiments.

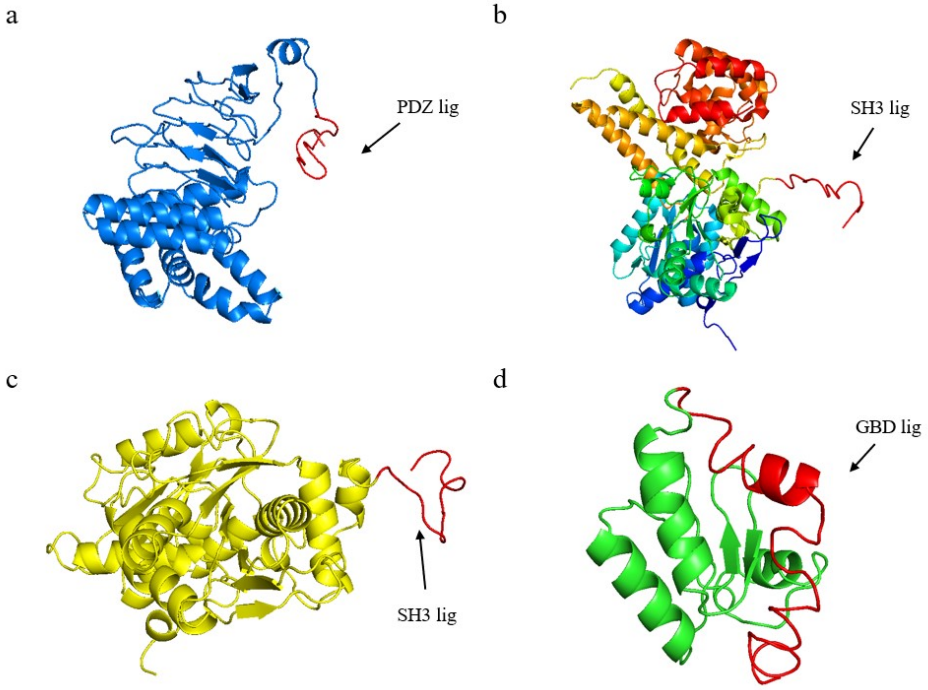

Supplementary Fig. 6. The monomer structure prediction results of protein scaffold ligand enzymes by homologous modeling. a Prediction of monomer structure of C-terminal connexin scaffold ligands in CysE**. b** Prediction of monomer structure of C-terminal connexin scaffold ligands in CysK. **c** Prediction of monomer structure of C-terminal connexin scaffold ligands in CysM. **d** Prediction of monomer structure of C-terminal connexin scaffold ligands in NrdH**.**

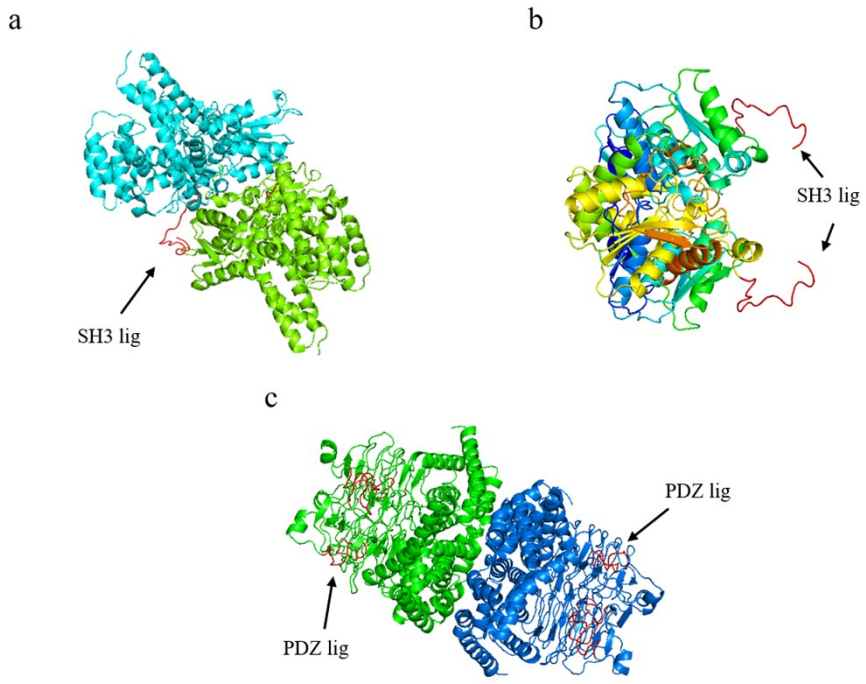

Supplementary Fig. 7. Predicted results of pathway enzyme multimers with protein scaffold ligand attached. a Prediction of dimer structure of C-terminal connexin scaffold ligands in CysK. **b** Prediction of dimer structure of C-terminal connexin scaffold ligands in CysM. **c** Prediction of hexamer structure of C-terminal connexin scaffold ligands in CysE.

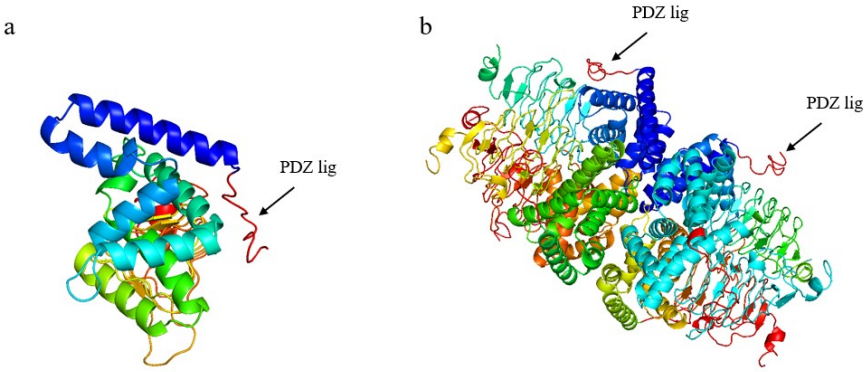

Supplementary Fig. 8. Prediction of monomer and polymer protein structure of N-terminal connexin scaffold ligands in CysE. a Prediction of monomer structure of N-terminal connexin scaffold ligands in CysE**. b** Prediction of hexamer structure of N-terminal connexin scaffold ligands in CysE.

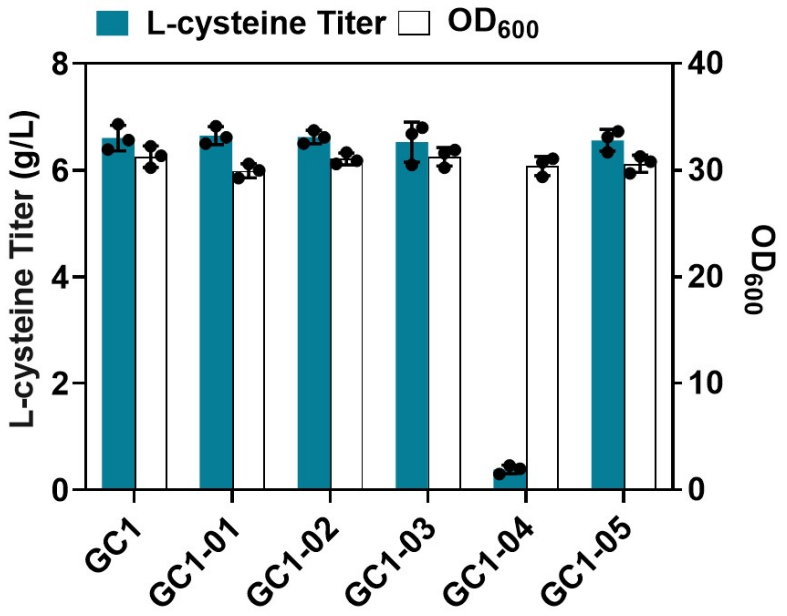

Supplementary Fig. 9. The effect of adding protein scaffold ligand to the pathway enzymes on cell growth and L-cysteine production. Based on the simulation prediction results of the key pathway enzyme structure model by I-Tasser, in order to verify the reliability of the simulation results, the protein scaffold ligands GBD lig, SH3 lig and SH3 lig were fused into the C-terminal of NrdH, CysK and CysM on the genome of strain GC1. The protein scaffold ligand PDZ lig was fused into the C-terminal and N-terminal of $CysE^{A237V}$ on the genome of strain GC1. Strains GC1-01 (GC1 derivative, NrdH-GBD lig), GC1-02 (GC1 derivative, CysK-SH3 lig), GC1-03 (GC1 derivative, CysM-SH3 lig), GC1-04 (GC1 derivative, $CysE^{A237V}$-PDZ lig C) and GC1-05 (GC1 derivative, $CysE^{A237V}$-PDZ lig N) were obtained. After 48 hours of shake flask fermentation, the titer of L-cysteine was determined and compared with the strain GC1 which did not express protein scaffold ligand, so as to determine the effect of ligand of protein scaffold on enzyme function.

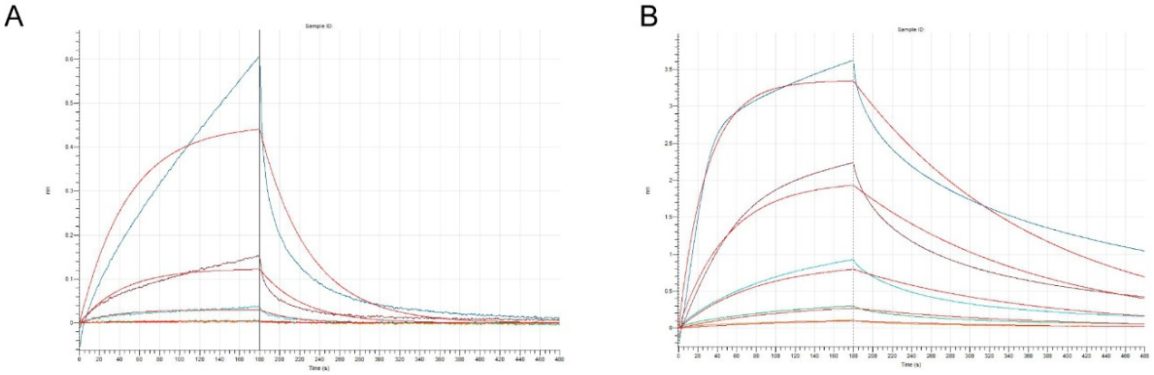

Supplementary Fig. 10. Fitting curve of combination and dissociation of P_{cysK} by CysB and $CysB^{V122G}$. A, cysB. B, $cysB^{V122G}$.

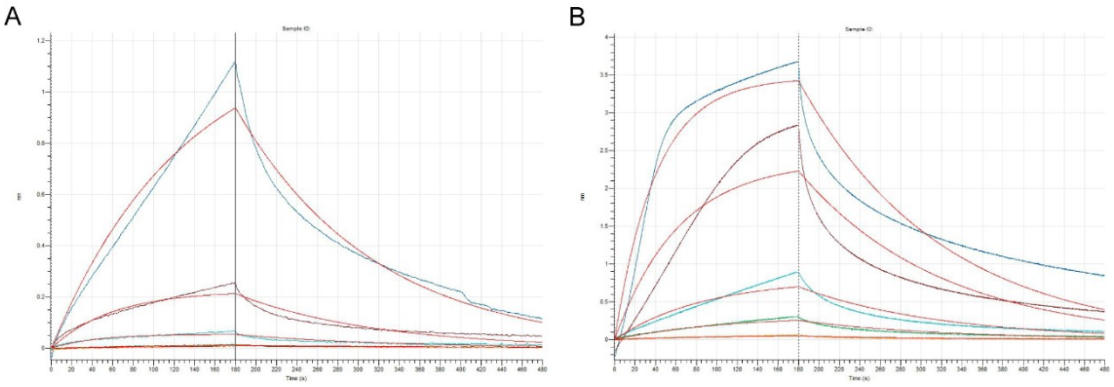

Supplementary Fig. 11. The combination and dissociation fitting curve of CysB and $CysB^{V122G}$ to P_{cysK} under external OAS. A, cysB. B, $cysB^{V122G}$.

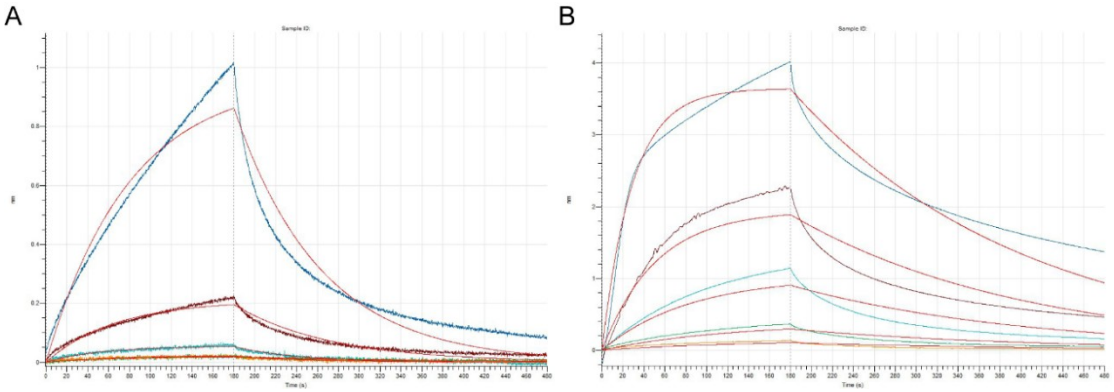

Supplementary Fig. 12. The binding and dissociation fitting curve of CysB and $CysB^{V122G}$ to P_{cysK} under the addition of sulfate. A, cysB. B, $cysB^{V122G}$.

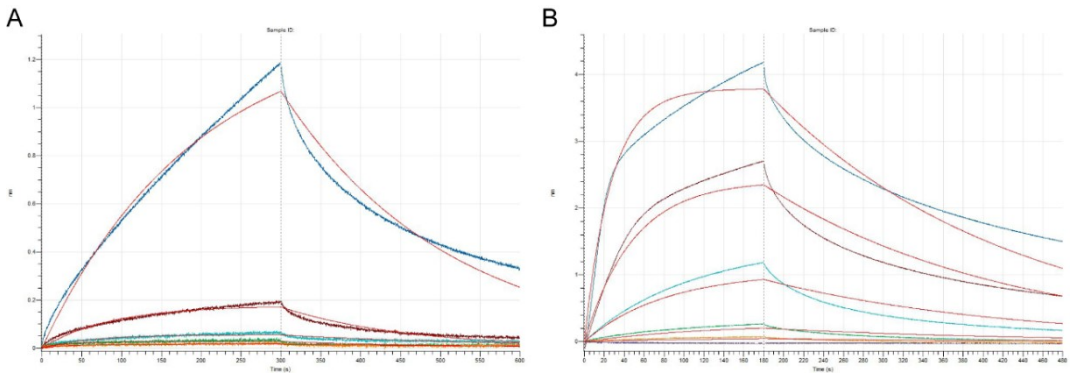

Supplementary Fig. 13. Binding and dissociation fitting curve of CysB and CysB^{V122G} to P_{cysK} under the addition of thiosulfate. A, cysB. B, cysB^{V122G}.

Supplementary Table 1. strains used in this study.

Strains	Description	Source
E. coli W3110	F$^-$, *λ-, IN* (*rrnD-rrnE*)*1, rph-1*	CGSC[a]
DH5α	F$^-$, *endA1*, *glnV44*, *thi-1*, *recA1*, *relA1*, *gyrA96*, *deoR*, *nupG*, *purB20*, φ80d*lacZ*, ΔM15, Δ(*lacZYA-argF*) U169, hsdR17(rK^-mK^+), λ^-	Tsingke
C1		Lab storage[1]
ΔydjN	C1, *ΔydjN*	This study
ΔyeaN	C1, *ΔyeaN*	This study
ΔfliY	C1, *ΔfliY*	This study
ΔydjNΔyeaN	C1, *ΔydjN*，*ΔyeaN*	This study
eamA	C1, Ptrc-*eamA*	This study
eamB	C1, Ptrc-*eamB*	This study
eamB^f	C1, Ptrc-$eamB^{G156S, N157S}$	This study
tolC	C1, Ptrc-*tolC*	This study
yijE	C1, Ptrc-*yijE*	This study
cydDC	C1, Ptrc-*cydDC*	This study
eamA-eamB^f	C1, Ptrc-*eamA*, Ptrc-$eamB^{G156S, N157S}$	This study
eamA-eamB^f-tolC	C1, Ptrc-*eamA*, Ptrc-$eamB^{G156S, N157S}$, Ptrc-*tolC*	This study
CS	C1, *ΔydjN*，*ΔyeaN* , Ptrc-*eamA*, Ptrc-$eamB^{G156S, N157S}$, Ptrc-*tolC*	This study
CS/pCysE^{f1}	CS/P_{trc}- $cysE^{L45Q/D250R}$, pTrc99a, Kan^R	This study
CS/pCysE^{f2}	CS/ P_{trc}- $cysE^{N12V/E39G}$, pTrc99a, Kan^R	This study
CS/pCysE^{f3}	CS/P_{trc}- $cysE^{V67M}$, pTrc99a, Kan^R	This study
CS/pCysE^{f4}	CS/P_{trc}- $cysE^{M201R}$, pTrc99a, Kan^R	This study
CS/pCysE^{f5}	CS/P_{trc}- $cysE^{T167A/G245S}$, pTrc99a, Kan^R	This study
CS/pCysE^{f6}	CS/P_{trc}- $cysE^{A237V}$, pTrc99a, Kan^R	This study
CS-Rtrc	CS derivative,*ΔyjiP-Ptrc-cysE^f*	This study
CS-R13	CS derivative,*ΔyjiP-R13-cysE^f*	This study
CS-R25	CS derivative,*ΔyjiP-R25-cysE^f*	This study
CS-R5	CS derivative,*ΔyjiP-R5-cysE^f*	This study

a: CGSC, Coli Genetic Stock Center.

Supplementary Table 1. strains used in this study (Continuation).

Strains	Description	Source
CS-R12	CS derivative,*ΔyjiP-R12-cysE*^{f}	This study
CS-R1	CS derivative,*ΔyjiP-R1-cysE*^{f}	This study
CS-R1-P13	CS-R1 derivative, *ΔyjiR-R13-cysE*^{f}	This study
CS-R1-P25	CS-R1 derivative, *ΔyjiR-R25-cysE*^{f}	This study
CS-R1-P5	CS-R1 derivative, *ΔyjiR-R5-cysE*^{f}	This study
CS-R1-P12	CS-R1 derivative, *ΔyjiR-R12-cysE*^{f}	This study
CS-R1-R1	CS-R1 derivative, *ΔyjiR-R1-cysE*^{f}	This study
CSE3	CS-R1-R1 derivative, *ΔyeeJ-cysE*^{f}	This study
CSE4	CS3 derivative, *ΔycdN-cysE*^{f}	This study
CSE5	CS4 derivative, *ΔydeU-cysE*^{f}	This study
CSE6	CS5 derivative, *ΔylbE-cysE*^{f}	This study
CSE7	CS6 derivative, *ΔyjhE-cysE*^{f}	This study
GC1	CSE7 derivative, *HflC-SerA*^{f}*, YbbK-SerC, HflK-SerB*	This study
GC1-1	GC1 derivative, eamA-*GBD*	This study
GC1-2	GC1 derivative, eamA-*GBD-SH3*	This study
GC2	GC1 derivative, *eamA-GBD-SH3-PDZ*	This study
GC2-1	GC2 derivative, *nrdH-GBD lig, cysK-SH3 lig, cysM-SH3 lig, cysE-PDZ lig*	This study
GC2-2	GC2 derivative, *nrdH-GBD lig, cysK-SH3 lig, cysE-PDZ lig*	This study
GC2-3	GC2 derivative, *nrdH-GBD lig, cysM-SH3 lig, cysE-PDZ lig*	This study
GCB1	GC2-3 derivative, *cysB 206TB*	This study
GCB2	GC2-3 derivative, *cysB 329TB*	This study
GCB3	GC2-3 derivative, *cysB 492TB*	This study
GCB4	GC2-3 derivative, *cysB 1016TB*	This study
GCB5	GC2-3 derivative, *cysB*^{Y164N} [4]	This study
GCB6	GC2-3 derivative, *cysB*^{A227D} [4]	This study
GCB7	GC2-3 derivative, *cysB*^{Q128L} [4]	This study

Supplementary Table 1. strains used in this study (Continuation).

Strains	Description	Source
GCB8	GC2-3 derivative, *cysB*^{T149M} [5]	This study
GCB9	GC2-3 derivative, *cysB*^{T149P} [5]	This study

Supplementary Table 2. Plasmids used in this study.

Plasmid	Description	Source
pTrc99a	pTrc99a, Kan^R	Lab storage
pCysE^{f1}	P_{trc}- *cysE*$^{L45Q/D250R}$, pTrc99a, Kan^R	Lab storage
pCysE^{f2}	P_{trc}- *cysE*$^{N12V/E39G}$, pTrc99a, Kan^R	This study
pCysE^{f3}	P_{trc}- *cysE*^{V67M}, pTrc99a, Kan^R	This study
pCysE^{f4}	P_{trc}- *cysE*^{M201R}, pTrc99a, Kan^R	This study
pCysE^{f5}	P_{trc}- *cysE*$^{T167A/G245S}$, pTrc99a, Kan^R	This study
pCysE^{f6}	P_{trc}- *cysE*^{A237V}, pTrc99a, Kan^R	This study
P-eGFP	pTrc99a, GFP; Kan^R	This study
RBS1	pTrc99a, GFP; Kan^R: GTATGATTATAAAAGTAAGGAGGTATTG RBS sequence	This study
RBS2	pTrc99a, GFP; Kan^R: GTATGTTGGCAAAAGTAAGGAGGTAATG RBS sequence	This study
RBS3	pTrc99a, GFP; Kan^R: GTATGTTCGCAAAAGTAAGGAGGTAGTG RBS sequence	This study
RBS4	pTrc99a, GFP; Kan^R: TTCACACAGGAAACC RBS sequence	This study
RBS5	pTrc99a, GFP; Kan^R: CGGAGGAAGAGGAGA RBS sequence	This study
RBS6	pTrc99a, GFP; Kan^R: ATTAAAGAGGAGAAA RBS sequence	This study
RBS7	pTrc99a, GFP; Kan^R: TCACACAGGAAACC RBS sequence	This study
RBS8	pTrc99a, GFP; Kan^R: TCACACAGGAAAG RBS sequence	This study
RBS9	pTrc99a, GFP; Kan^R: TCACACAGGAC RBS sequence	This study
RBS10	pTrc99a, GFP; Kan^R: ATTAAAGAGGAGAA RBS sequence	This study
RBS11	pTrc99a, GFP; Kan^R: AAAGAGGAGAAA RBS sequence	This study
RBS12	pTrc99a, GFP; Kan^R: AAAGAGGGGAAA RBS sequence	This study
RBS13	pTrc99a, GFP; KanR: AAAGAAGGGATAC RBS sequence	This study
RBS14	pTrc99a, GFP; KanR: AAGGAG RBS sequence	This study
RBS15	pTrc99a, GFP; KanR: AAGAAGGAGATATACAT RBS	This study

sequence

Supplementary Table 2. Plasmids used in this study (Continuation).

Plasmid	Description	Source
RBS16	pTrc99a, GFP; Kan^R: AATAATTTTGTTTAACTTTAAGAAGGAGAT RBS sequence	This study
RBS17	pTrc99a, GFP; Kan^R: AAAGAGGTGACA RBS sequence	This study
RBS18	pTrc99a, GFP; Kan^R: AAAGAGACGAG RBS sequence	This study
RBS19	pTrc99a, GFP; Kan^R: AAAGAGGCGATA RBS sequence	This study
RBS20	pTrc99a, GFP; Kan^R: AAAGACGAGATA RBS sequence	This study
RBS21	pTrc99a, GFP; Kan^R: AAAGATATGAAT RBS sequence	This study
RBS22	pTrc99a, GFP; Kan^R: AAAGACATGAGT RBS sequence	This study
RBS23	pTrc99a, GFP; Kan^R: AAAGACCCGAGA RBS sequence	This study
RBS24	pTrc99a, GFP; Kan^R: AAAGACGCGAG RBS sequence	This study
RBS25	pTrc99a, GFP; Kan^R: AAAGAGGGCACA RBS sequence	This study
Ptrc-RBS	pTrc99a, GFP; Kan^R: TTTCACACAGGAAACAGACC RBS sequence	This study

Supplementary Table 3. Topological domain and transmembrane characteristics of EamA.

Type	Location	Description
Topological domain	1-6	Cytoplasm
Transmembran	7-27	Screw
Topological domain	28-31	Periprime space
Transmembran	32-52	Screw
Topological domain	53-59	Cytoplasm
Transmembran	60-80	Screw
Topological domain	81-87	Periprime space
Transmembran	88-108	Screw
Topological domain	109-116	Cytoplasm
Transmembran	117-137	Screw
Topological domain	138-140	Periprime space
Transmembran	141-161	Screw
Topological domain	162-175	Cytoplasm
Transmembran	176-196	Screw
Topological domain	197-216	Periprime space
Transmembran	217-237	Screw
Topological domain	238-243	Cytoplasm
Transmembran	244-264	Screw
Topological domain	265-268	Periprime space
Transmembran	269-289	Screw
Topological domain	290-299	Cytoplasm

Supplementary Table 4. Topological domain and transmembrane characteristics of EamB.

Type	Location	Description
Topological domain	1-7	Periprime space
Transmembran	8-28	Screw
Topological domain	29-46	Cytoplasm
Transmembran	47-67	Screw
Topological domain	68-69	Periprime space
Transmembran	70-90	Screw
Topological domain	91-104	Cytoplasm
Transmembran	105-125	Screw
Topological domain	126-141	Periprime space
Transmembran	142-162	Screw
Topological domain	163-176	Cytoplasm
Transmembran	177-194	Screw
Topological domain	195	Periprime space

Supplementary Table 5. Binding motifs of regulatory transcription factor CysB to target genes.

Target gene	Regulatory level	Binding motif
cysB	Repression	TGGTTATAGTTAGCA
hslJ	Repression	CTATTCTTAAAATAG
cysDNC	Activation	GCTTTGCCAAATCGT
cysJIH	Activation	AGGTTAGTCGATTTG
cysK	Activation	TTATTTCCCTTCTGT
cysPU	Activation	CCGTTACTCCTTTCA
tauABCD	Activation	TAATTGCATATTTAA

we compiled binding motifs for CysB positively regulated genes (Supplementary Table 5), performed sequence comparisons of the binding regions through the MetaLogo website, and characterized the interaction between regulatory protein CysB and its corresponding active DNA binding sequences.

Supplementary Table 6. Sequencing results of mutant loci for different mutants.

Mutant name	Mutation site
206TB	I112P、I134N、W166C、F222M、I230T、V251A、R290C
329TB	V122G
692TB	R105H、L178Q、S277T
1016TB	F279L

Supplementary references

1. J. Ostrowski and N. M.Kredich, *J. Bacteriol.*, 1991, **173**, 2212–2218.

2. J. Ostrowski and N. M. Kredich, *J. Bacteriol.*, 1990, **172**, 779–785.

3. C. Monroe, W. Swann, H. Robinson and C. Wieman, *Phys. Rev. Lett.*, 1990, **65**, 1571–1574.

4. A. Lochowska, R. Iwanicka-Nowicka, D. Plochocka, and M. M. Hryniewicz, *J. Biol. Chem.*, 2001, **276**, 1893–1900.

5. T. E. Colyer and N. M. Kredich, *Mol. Microbiol.*, 1996, **21**, 197–206.